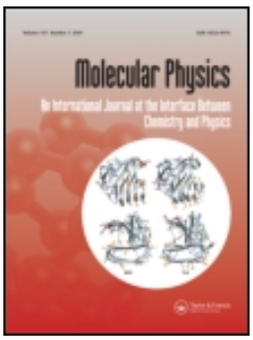

Molecular Physics

ISSN: 0026-8976 (Print) 1362-3028 (Online) Journal homepage: http://www.tandfonline.com/loi/tmph20

Microwave spectrum of the $K_a = 1 \leftarrow 0$ rotation-tunnelling band of $(D_2O)_2$

E.N. Karyakin , G.T. Fraser & R.D. Suenram

To cite this article: E.N. Karyakin , G.T. Fraser & R.D. Suenram (1993) Microwave spectrum of the $K_a = 1 \# 0$ rotation-tunnelling band of $(D_2O)_2$, Molecular Physics, 78:5, 1179-1189, DOI: 10.1080/00268979300100771

To link to this article: http://dx.doi.org/10.1080/00268979300100771

MOLECULAR PHYSICS, 1993, VOL. 78, No. 5, 1179–1189

Microwave spectrum of the $K_a = 1 \leftarrow 0$ rotation-tunnelling band of $(D_2O)_2$

By E. N. KARYAKIN
Molecular Spectroscopy Laboratory, Applied Physics Institute, Nizhnii Novgorod, Russia

G. T. FRASER and R. D. SUENRAM
Molecular Physics Division, National Institute of Standards and Technology, Gaithersburg, MD 20899, USA

(*Received 1 September 1992; accepted 7 September 1992*)

A 78–118 GHz synthesizer-driven backward-wave oscillator is used together with klystron sources and frequency doublers to measure the electric-resonance optothermal spectrum of the $K_a = 1 \leftarrow 0$ rotation-tunnelling subband of $(D_2O)_2$. Transitions are observed originating from each of the six tunnelling states, A_1^+, B_1^+, E_1^+, A_2^-, B_2^-, and E_2^-, allowing an estimate of the largest tunnelling matrix element h_{4v}, characterizing the separation of the A_1^+, B_1^+, and E_1^+ states from the A_2^-, B_2^-, and E_2^- states. We find the average of h_{4v} for the $K_a = 0$ and 1 states to be $\sim -8\,943$ MHz. A comparison of the $K_a = 1 \leftarrow 0$ band origins for the A/B states with the band origin for their E partner gives $h_{2v} \sim -6{\cdot}9$ MHz, where h_{2v} is the tunnelling matrix element responsible for the displacement of the E symmetry levels from the center of their interconversion split A/B partners. Values found for the A rotational constant, $A \sim 124\,923$ MHz, and h_{2v} are in good agreement with those obtained from the submillimetre measurements of Zwart, E., ter Meulen, J. J., and Meerts, W. L., 1990, *Chem. Phys. Lett.*, **173**, 115, on the $K_a = 2 \leftarrow 1$ band of the complex. Estimates are presented for the potential barriers to the $1 \rightarrow 2$, $1 \rightarrow 5$ and $1 \rightarrow 7$ tunnelling processes.

1. Introduction

The importance of H_2O in many condensed-phase processes has led to an extensive experimental [1–18] and theoretical [19–24] effort at characterizing the high-resolution microwave [1–12], far-infrared [13–16], and infrared [17, 18] spectra of $(H_2O)_2$. The microwave spectrum of $(H_2O)_2$ gives a hydrogen-bonded C_s-symmetry structure in which facile tunnelling between isoenergetic configurations allows each of the hydrogens to participate in the hydrogen bonding. The tunnelling splittings present in the normal $(H_2O)_2$ species are as large as 150–200 GHz, and show substantial evidence for coupling between the rotation and tunnelling degrees of freedom. Because of this, the spectroscopic constants extracted from any spectral analysis will be contaminated considerably from tunnelling effects, unless a proper treatment of the rotation-tunnelling dynamics is used. Indeed, efforts have been made in this direction by Coudert and Hougen [20, 22, 24], who have used their internal-axis-like method to fit the spectroscopic data for the $(H_2O)_2$ isotopic form.

The Coudert and Hougen analysis shows [24], however, that a high-barrier internal axis method (IAM) may not be appropriate for the totally protonated

0026-8976/93 $10.00

species where the tunnelling splittings are a significant fraction of the barrier height. For this reason it is important to study the deuterated forms of the dimer, where the more massive deuterium nuclei lead to substantially reduced tunnelling splittings. Along these lines, for $(D_2O)_2$, *a* type $\Delta K_a = 0$ microwave transitions have been reported for $K_a = 0$ and 1 by Dyke *et al.* [2], Odutola *et al.* [3, 6], Coudert *et al.* [4], and Suenram *et al.* [9] and *c* type $K_a = 2 \leftarrow 1$ submillimetre transitions have been observed by Zwart *et al.* [15]. In addition, Pugliano and Saykally [16] have observed a fundamental vibration of the dimer near $84\,cm^{-1}$. Together, these measurements determine many of the smaller tunnelling splittings in $(D_2O)_2$ but provide little information about the largest tunnelling splitting resulting from the interchange of the two deuterium nuclei on the proton-acceptor unit.

In the present paper, we report our observation of the *c* type $K_a = 1 \leftarrow 0$ band of $(D_2O)_2$, recorded using an electric-resonance optothermal spectrometer (EROS) [8, 9, 11]. These measurements allow us to obtain an estimate of $\sim 36\,GHz$ for the largest tunnelling splitting in the dimer. In addition, we find a value for the *A* rotational constant for the complex which is in good agreement with an estimate obtained by Zwart *et al.* [15] from their investigation of the $K_a = 2 \leftarrow 1$ band of the dimer, suggesting that this *A* value is essentially uncontaminated by tunnelling effects and thus should be useful in a structural analysis. Finally, we use the measured tunnelling matrix elements for the $1 \rightarrow 2$, $1 \rightarrow 5$ and $1 \rightarrow 7$ pathways to estimate the tunnelling barriers and vibrational frequencies associated with these motions.

2. Experimental

The microwave spectrum of the $K_a = 1 \leftarrow 0$ band of $(D_2O)_2$ was measured using an electric-resonance optothermal spectrometer described previously in our studies of $(H_2O)_2$ [8, 11] and $(D_2O)_2$ [9]. Briefly, an inhomogeneous electrostatic field of quadrupolar symmetry is used to focus or direct a molecular beam of $(D_2O)_2$ onto a liquid helium cooled bolometer detector [25]. Prior to the quadrupole field, the molecules are interrogated by a microwave field which is 100% amplitude or tone-burst modulated [26] at $\sim 400\,Hz$. The synchronous output from the bolometer is monitored with a phase-sensitive amplifier to look for a modulation of the focused beam intensity, which results when the microwave field is resonant with a molecular transition.

For a transition to be observed it is necessary that one of the two states involved in the transition has a positive Stark coefficient, so that molecules in that state can be focused by the quadrupole field onto the detector. Thus, in addition to the usual Hönl–London and Boltzmann factors, the transition intensities also depend strongly on the focusing characteristics of the upper and lower states of the transitions.

In the present investigation, two new microwave sources were used. Broad-banded scans were facilitated by using a backward-wave oscillator which was phase locked to a microprocessor-controlled frequency synthesizer developed in Nizhnii Novgorod, Russia [27]. With this unit, uninterrupted scans were made in the 78–118 GHz region. Measurements above 120 GHz were made using a frequency doubler, which was driven by 55–85 GHz phase-locked klystrons. While undertaking the experiments, spectra were also observed and assigned for the $K_a = 1 \leftarrow 0$ band of HOD--DOD. These results will be reported in a later paper [28].

3. Summary of theory

Dyke has shown [19] by application of the molecular symmetry group G_{16} (appropriate if no tunnelling pathways are allowed which break covalent bonds) that hydrogen tunnelling splits each of the rigid-rotor energy levels of $(H_2O)_2$ into six components. For rotational levels of A′ symmetry in C_s, rotational-tunnelling levels of A_1^+, B_1^+, E^+, A_2^-, B_2^-, and E^- symmetry in G_{16} result; for A″ rotational levels, the rotational-tunnelling species are of A_1^-, B_1^-, E^-, A_2^+, B_2^+, and E^+ symmetry. Here, the +/− superscripts denote the symmetry of the wavefunction under the inversion operation E^*. The largest tunnelling splitting, denoted $1 \rightarrow 4$ in the notation of Hougen [20], corresponds to interchanging the two hydrogens on the proton acceptor H_2O unit, and separates the $A_1^\pm$, $B_1^\pm$, and $E^\pm$ states from the $A_2^\mp$, $B_2^\mp$, and $E^\mp$ states. The $A_1^\pm$ and $B_1^\pm$ states are symmetrically split from their $E^\pm$ partner states by the interconversion tunnelling matrix elements, h_{5v} and h_{7v}, as are the $A_2^\mp$ and $B_2^\mp$ states split from their $E^\mp$ partner. The E states are slightly displaced from the centre of their A/B partners by the h_{2v} matrix element. For convenience we will denote the $E^\pm$ states associated with the $A_1^\pm$ and $B_1^\pm$ states as $E_1^\pm$ and the $E^\pm$ states associated with the $A_2^\pm$ and $B_2^\pm$ states as $E_2^\pm$.

The tunnelling matrix elements h_{5v}, h_{7v}, and h_{2v} are associated with tunnelling paths $1 \rightarrow 5$, $1 \rightarrow 7$, and $1 \rightarrow 2$ in the convention of Coudert and Hougen, where $1 \rightarrow 5$ corresponds to a geared interchange of the proton-donor and proton-acceptor units, $1 \rightarrow 7$ corresponds to an antigeared interchange of the donor and acceptor units, and $1 \rightarrow 2$ corresponds to an interchange of the two deuterium nuclei on the proton donating unit and an interchange of the two deuterium nuclei on the proton acceptor unit.

The electric dipole selection rules on the rotation-tunnelling species are:

$$A_1^+ \leftrightarrow A_1^-$$

$$B_1^+ \leftrightarrow B_1^-$$

$$A_2^+ \leftrightarrow A_2^-$$

$$B_2^+ \leftrightarrow B_2^-$$

$$E^+ \leftrightarrow E^-,$$

and the nuclear-spin statistical weights for the totally deuterated species are:

$$A_1^\pm \quad 21$$

$$B_1^\pm \quad 15$$

$$E^\pm \quad 18$$

$$A_2^\pm \quad 3$$

$$B_2^\pm \quad 6.$$

Consideration of previous work on $(H_2O)_2$ and $(D_2O)_2$ leads to the energy level diagram for $(D_2O)_2$ given in figure 1. The subject of the present study is the six $K_a = 1 \leftarrow 0$ subbands shown with a "?" in the figure, and assumed by analogy with the results of $(H_2O)_2$ to have the selection rules as drawn.

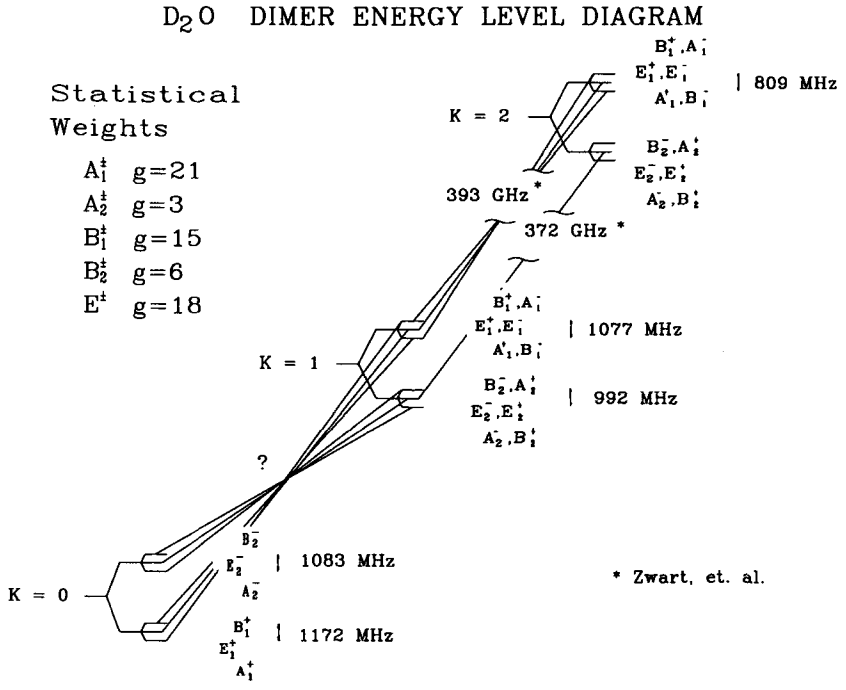

Figure 1. Energy level diagram for $(D_2O)_2$. The $K = 1 \leftarrow 0$ subbands shown with a "?" are the subject of the present study.

4. Results

The observed transitions for the $K_a = 1 \leftarrow 0$ band of $(D_2O)_2$ dimer are presented in table I. The assignment of the transitions to this subband is based, in part, on precise ground ($K_a = 0$) and excited-state ($K_a = 1$) combination differences obtained from the previous studies [4, 9, 15] of $(D_2O)_2$. A total of six subbands is observed; two originating from the two symmetric interconversion tunnelling states, A_1^+ and A_2^-, two from the two antisymmetric interconversion tunnelling states, B_1^+ and B_2^-, and two from the two doubly degenerate noninterconverting states, E_1^+ and E_2^-. Here, the species labels refer to the tunnelling-state symmetries and not to the overall rotation-tunnelling symmetries. The six subbands are independently fit to the frequency expression,

$$\nu = \nu_0 + \bar{B}_{K=1}[J'(J'+1) - K_a'^2] - D_{K=1}[J'(J'+1) - K_a'^2]^2 + (-1)^{K_a'+K_c'+J'} \frac{(B-C)_{K=1}}{4} J'(J'+1) - \bar{B}_{K=0} J''(J''+1) + D_{K=0}[J''(J''+1)]^2, \quad (1)$$

where $\bar{B} = (B+C)/2$. For a c type band, the Q-branch lines terminate on $K_a' = 1$ levels having $K_a' + K_c' + J'$ odd, while the P- and R-branch lines terminate on $K_a' = 1$ levels having $K_a' + K_c' + J'$ even. Included in the fits are a type, $\Delta K_a = 0$ combination differences generated from the microwave data summarized in table I of Suenram *et al.* [9]. The spectroscopic constants resulting from the fits are listed in table 2. Here, we have constrained the $D_{K=0}$ and $D_{K=1}$ centrifugal distortion constants to be equal. The standard deviations from the fits range from 0·06 to 0·31 MHz.

Table 1. Observed microwave transition frequencies for the $K_a = 1 \leftarrow 0$ band of $(D_2O)_2$ (in MHz).

	A_1^+ [a]	E_1^+	B_1^+	A_2^-	E_2^-	B_2^-
P(7)	80750·91	79620·90				
P(6)	91495·80	90359·82	89276·73			
P(5)	102263·05	101122·13		30718·50	29661·32	
P(4)	113051·75	111906·70	110815·40	41473·39	40413·02	
Q(1)	156385·64		154138·53			
Q(2)	156353·37	155203·41	154109·28	84670·16	83605·51	82594·76
Q(3)	156304·88	155157·42	154065·46	84568·01	83504·80	
Q(4)	156240·39	155096·24	154007·11	84431·90		
Q(5)	156159·89					
R(0)	167283·51	166131·50		95662·49	94596·78	
R(1)				106577·40	105512·72	
R(2)				117515·90	116453·10	

[a] Tunnelling-state symmetry for the lower state of the rotation-tunnelling subband.

5. Discussion

The present measurements on the $K_a = 1 \leftarrow 0$ band of $(D_2O)_2$ furnish information on the A rotational constant and the tunnelling matrix elements h_{2v} and h_{4v} of Coudert and Hougen [20, 22, 24]. Following Coudert and Hougen, we will take all the $h_{iv} < 0$ to insure that the totally symmetric state is lowest in energy. The weighted average (to account for the doubly degenerate E_1^+ state) of the subband origins for the A_1^+, B_1^+, and E_1^+ tunnelling states (table 2) gives,

$$A + 2|h_{4v}^{K=0}| + 2|h_{4v}^{K=1}| = \tfrac{1}{4}[\nu_0(A_1^+) + \nu_0(B_1^+) + 2\nu_0(E_1^+)], \tag{2}$$

whereas the weighted average of the subband origins for the A_2^-, B_2^-, and E_2^- tunnelling states gives,

$$A - 2|h_{4v}^{K=0}| - 2|h_{4v}^{K=1}| = \tfrac{1}{4}[\nu_0(A_2^-) + \nu_0(B_2^-) + 2\nu_0(E_2^-)]. \tag{3}$$

Here, $h_{4v}^{K=0}$ and $h_{4v}^{K=1}$ are the values of h_{4v} for the $K_a = 0$ and 1 states, respectively, where h_{4v} is the largest of the tunnelling matrix elements in $(D_2O)_2$, and arises from the interchange of the two deuterium nuclei on the proton-acceptor D_2O unit. From equations (4) and (5) we find $A = 124{\cdot}9$ GHz and $[|h_{4v}^{K=0}| + |h_{4v}^{K=1}|]/2 = 8\,943$ MHz. This value for A agrees well with that determined by Zwart *et al.* [15] who find $A = 125{\cdot}8$ GHz from an analysis of the $K_a = 2 \leftarrow 1$ band of the dimer. We note that our observations verify the Zwart *et al.* preferred ordering of the $1 \rightarrow 2$ tunnelling splittings for the $K_a = 1$ and 2 states.

Information is also available on the h_{2v} matrix element, which arises from a tunnelling process that interchanges the two deuterium nuclei on the proton acceptor and the two deuterium nuclei on the proton donor. If we assume that h_{2v} is independent of K_a, then we find that,

$$-4h_{2v} = \frac{[\nu_0(A_1^+) + \nu_0(B_1^+)]}{2} - \nu_0(E_1^+) \tag{4}$$

Table 2. Spectroscopic constants for the $K_a = 1 \leftarrow 0$ band of $(D_2O)_2$ (in MHz).

	A_1^+ [a]	E_1^+	B_1^+	A_2^-	E_2^-	B_2^-
ν_0	161834·409(48)[b]	160682·29(19)	159586·00(22)	90202·604(32)	89136·62(16)	88124·58(15)
$\bar{B}_{K=1}$	5432·7014(48)	5432·941(20)	5433·057(19)	5430·2859(61)	5430·476(21)	5430·544(16)
$D_{K=1}$	0·03712(20)	0·03755(12)	0·03748(93)	0·03535(26)	0·037687(98)	0·03598(73)
$(B-C)_{K=1}$	33·0026(92)	33·100(30)	33·065(37)	59·4142(67)	59·620(43)	59·746(23)
$\bar{B}_{K=0}$	5432·5871(66)	5432·396(17)	5432·159(28)	5432·5228(69)	5432·420(12)	5432·220(17)
$D_{K=0}$	0·03712(20)	0·03755(12)	0·03748(93)	0·03535(26)	0·037687(98)	0·03598(73)
σ[c]	0·087	0·28	0·31	0·058	0·25	0·14

[a] Tunnelling-state symmetry for the lower-state of the rotation-tunnelling subband.
[b] The numbers in parentheses are the uncertainties and represent one standard error from the fit in units of the least significant digit shown.
[c] Standard deviation of the least-squares fit in MHz.

and

$$-4h_{2v} = \frac{[\nu_0(A_2^-) + \nu_0(B_2^-)]}{2} - \nu_0(E_2^-). \quad (5)$$

These expressions give $h_{2v} = -7{\cdot}0$ and $-6{\cdot}7$ MHz for the $A_1^+/E_1^+/B_1^+$ and the $A_2^-/E_2^-/B_2^-$ subbands, respectively. From their analysis of the $K_a = 2 \leftarrow 1$ band of the dimer, Zwart *et al.* [15] find $h_{2v} = -6{\cdot}4$ MHz, suggesting that h_{2v} has only a very weak K_a dependence. Finally, the observed selection rules on the h_{2v} tunnelling splitting (i.e., symmetric $\leftrightarrow$ antisymmetric for the c type $\Delta K = 1$ spectrum) indicates that the c component of the dipole moment μ_c is an antisymmetric function of the $1 \rightarrow 2$ tunnelling coordinate. This is consistent with the tunnelling pathway chosen by Coudert and Hougen [22] after consideration of the semiempirical $(H_2O)_2$ potential of Coker and Watts [29]. The observed tunnelling-state selection rule on h_{2v} is inconsistent with a tunnelling pathway corresponding to the internal rotation of each water unit 180° about its C_2 axis, since here the c dipole component would be a symmetric function of the tunnelling coordinate. The observed selection

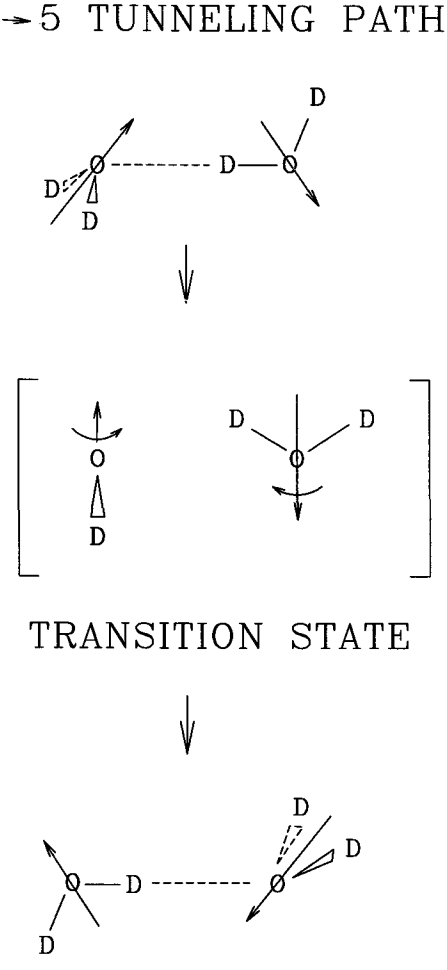

Figure 2. Simplified model of the $1 \rightarrow 5$ tunnelling process as a geared internal rotation of the two H_2O units about their C_2 axes.

rules for the $1 \rightarrow 5$, $1 \rightarrow 7$, and $1 \rightarrow 4$ splittings also indicate that these tunnelling processes lead to a reversal of the direction of the μ_c dipole moment component in the molecular frame. In the case of the $1 \rightarrow 4$ splitting, the selection rules are not as clear because of the large coupling of the tunnelling motion with the K_a rotation, which leads to a large decrease with K_a of the $1 \rightarrow 4$ splitting so that by $K_a = 2$, the order of the symmetric and antisymmetric states has been reversed.

The present data on $(D_2O)_2$, together with previous measurements on both $(D_2O)_2$ and $(H_2O)_2$, give substantial information on the tunnelling dynamics of the water dimer, provided methods exist to extract barriers and tunnelling pathways from the observed splittings. If we assume that the model of Coudert and Hougen [22] is appropriate for the $(D_2O)_2$, i.e., that the tunnelling splittings are small compared with the vibrational frequencies, then each of the tunnelling matrix elements h_{iv} can be related approximately to a 1-dimensional slice through the water dimer potential energy surface. With an appropriate 1-dimensional tunnelling model, the observed tunnelling matrix elements can be used to estimate the barriers for the various tunnelling processes. Here, we will model the three tunnelling motions, $1 \rightarrow 5$, $1 \rightarrow 7$, and $1 \rightarrow 2$, associated with the tunnelling matrix elements h_{5v}, h_{7v}, and h_{2v}, by 1-dimensional tunnelling models similar to those used in the treatment of the interchange tunnelling in $(HCCH)_2$ [30] and $(HF)_2$ [31].

To simulate the $1 \rightarrow 5$ tunnelling process we deform the $(D_2O)_2$ dimer slightly so that the two D_2O units have their C_2 axes antiparallel as shown in figure 2. Using this structure, the geared $1 \rightarrow 5$ motion can be pictured as a concerted geared internal rotation of the two H_2O units about their C_2 symmetry axes. The transition state in this case resembles qualitatively the C_i transition state found in the *ab initio* calculations of Smith *et al.* [23]. With this model, the tunnelling problem in $(H_2O)_2$ becomes essentially identical to the internal-rotation-like interconversion problem in acetylene dimer [30], where the approximate tunnelling Hamiltonian takes the form,

$$Fp^2 + \frac{V_4}{2}(1 - \cos 4\alpha), \tag{6}$$

where V_4 is the barrier to interconversion, α is the internal-rotation angle, $p = -i\partial/\partial\alpha$, and $F = b_0/2$. Here, b_0 is the zero-point B rotational constant of D_2O or H_2O. For D_2O, $b_0 = 7{\cdot}27\,\text{cm}^{-1}$, for H_2O, $b_0 = 14{\cdot}52\,\text{cm}^{-1}$. We find that values of $V_4 = 405\,\text{cm}^{-1}$ and $447\,\text{cm}^{-1}$ reproduce the observed $1 \rightarrow 5$ h_{5v} tunnelling matrix elements of $-281{\cdot}9$ MHz [9] and $-5260{\cdot}9$ MHz [8] for $(D_2O)_2$ and $(H_2O)_2$, respectively. Smith *et al.* [23] determine from their *ab initio* calculations (MP4/6 − 311 + G(2df, 2p)) a barrier of $304\,\text{cm}^{-1}$ for the $1 \rightarrow 5$ motion, substantially lower than the values found above. One possible source of error in our model that would lead to an overestimate of the tunnelling barrier is the use of too small a reduced mass for the tunnelling process. For instance, if the $1 \rightarrow 5$ tunnelling process also requires some partial rotation about the c inertial axes of the individual water units, this would lead to an increase in the effective reduced mass for tunnelling and, thus, a smaller F value in the present model.

In a similar manner, we picture the $1 \rightarrow 7$ tunnelling pathway as the antigeared version of the $1 \rightarrow 5$ tunnelling process. As before, we use equation (6) with the same F values as used for the $1 \rightarrow 5$ calculations. A barrier height of $741\,\text{cm}^{-1}$ is obtained by fitting the observed [9] h_{7v} tunnelling matrix element of $-11{\cdot}1$ MHz. For $(H_2O)_2$, the $741\,\text{cm}^{-1}$ barrier implies an h_{7v} tunnelling matrix element of -829 MHz, compared with the observed value [8] of -378 MHz. A barrier of $883\,\text{cm}^{-1}$ for the

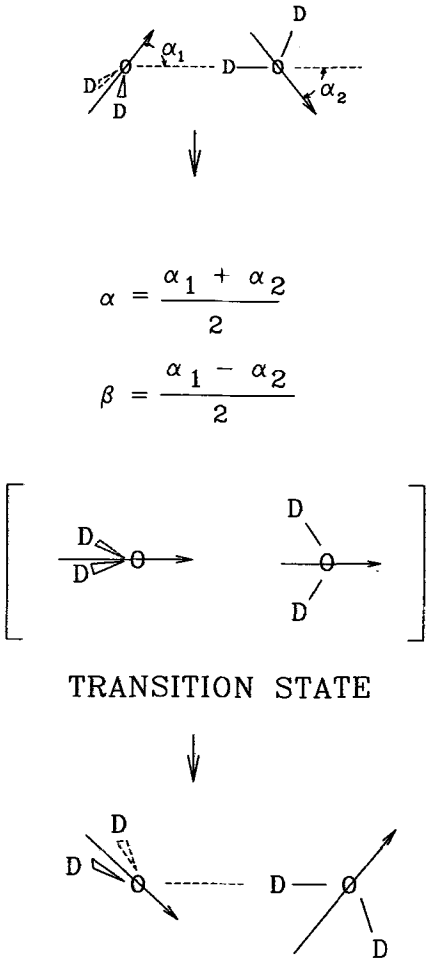

Figure 3. The $1 \rightarrow 2$ tunnelling process modelled as a simultaneous hindered rotation of the proton-acceptor unit about its *a* inertial axis and the proton-donor unit about its *c* inertial axis. The tunnelling motion is assumed to move along a path in which $\alpha \rightarrow -\alpha$ and $\beta \sim 0$.

$(H_2O)_2$ gives the correct h_{7v} value for this species.

To model the $1 \rightarrow 2$ tunnelling process we consider a quartic potential [31, 32] of the form,

$$V(\alpha) = V_b\left[\left(\frac{\alpha}{\alpha_e}\right)^4 - 2\left(\frac{\alpha}{\alpha_e}\right)^2\right] \tag{7}$$

where V_b is the barrier to tunnelling, α is the tunnelling coordinate and α_e is the equilibrium value of α. Following Smith *et al.* [23] and Coudert and Hougen [22], we take the tunnelling pathway to correspond to a simultaneous partial rotation of the proton acceptor unit about its *a* inertial axis and the proton donor about its *c* inertial axis, as pictured in figure 3. The kinetic energy operator is the same as in equation (6), but with $2F = (1/a_0 + 1/c_0)^{-1}$, where $a_0 = 15{\cdot}42\,\text{cm}^{-1}$ and $c_0 = 4{\cdot}85\,\text{cm}^{-1}$ are the zero-point *A* and *C* rotational constants of D_2O. For H_2O, $a_0 = 27{\cdot}88\,\text{cm}^{-1}$ and $c_0 = 9{\cdot}28\,\text{cm}^{-1}$. Considering an idealized $(D_2O)_2$ structure with the $O\cdots D{-}O$ bond

essentially linear and directed along one of the unoccupied sp^3 hybrid orbitals of the proton donor leads us to approximate α_e as $\angle DOD./2 = 52°$, where $\angle DOD$ is the bond angle of D_2O. With these approximations we find that a barrier of $592\,cm^{-1}$ reproduces the observed h_{2v} matrix element of $-6{\cdot}9$ MHz. For $(H_2O)_2$ a $592\,cm^{-1}$ barrier implies an h_{2v} matrix element of -505 MHz compared with the observed value of -743 MHz [8]. A barrier of $545\,cm^{-1}$ for $(H_2O)_2$ gives the correct tunnelling splitting for this species. The calculations of Smith *et al.* give a barrier of $658\,cm^{-1}$ for the $1 \rightarrow 2$ tunnelling.

The barrier calculations presented above also allow us to estimate the frequencies of the three fundamental vibrational bands associated with the three large amplitude motions analysed. For the $A''C_s$ vibrations of $(D_2O)_2$ arising from the $1 \rightarrow 5$ and $1 \rightarrow 7$ motions we estimate vibrational frequencies of 137 and $192\,cm^{-1}$, respectively, with corresponding excited state tunnelling matrix elements of $h_{5v} = +8802$ MHz and $h_{7v} = +513$ MHz. For the A' vibration associated with the $1 \rightarrow 2$ tunnelling process in $(D_2O)_2$ we estimate a frequency of $191\,cm^{-1}$ and a tunnelling matrix element $h_{2v} = -927$ MHz.

In conclusion, the present measurements of the K_a $1 \leftarrow 0$ band of $(D_2O)_2$ provide improved estimates for the A rotational constant and the h_{2v} and h_{4v} tunnelling matrix elements of the dimer. We have also presented simple models to estimate potential barriers and vibrational frequencies associated with some of the tunnelling motions. Hopefully, these efforts, together with the large base of spectroscopic data available on the water dimer, will motivate renewed theoretical initiatives to obtain an experimental intermolecular potential for the water dimer interaction, such has been undertaken successfully for the well characterized rare-gas hydrogen halides and $(HF)_2$ systems.

We would like to thank Laurant Coudert for sending us his predictions for the $K_a = 1 \leftarrow 0$ band of $(D_2O)_2$, Nick Pugliano and Jon Hougen for numerous stimulating discussions during the course of this work, and A. A. Ulyanov and O. P. Pavlovsky of NNIPI in Nizhnii Novgorod, Russia for the generous loan of the synthesizer-drived BWO system used in this work.

References

[1] Dyke, T. R., and Muenter, J. S., 1974, *J. chem. Phys.*, **60**, 2929.
[2] Dyke, T. R., Mack, K. M., and Muenter, J. S., 1977, *J. chem. Phys.*, **66**, 498.
[3] Odutola, J. A., and Dyke, T. R., 1980, *J. chem. Phys.*, **72**, 5062.
[4] Coudert, L. H., Lovas, F. J., Suenram, R. D., and Hougen, J. T., 1987, *J. chem. Phys.*, **87**, 6290.
[5] Dyke, T. R., 1987, *Structure and Dynamics of Weakly Bound Molecular Complexes*, edited by A. Weber (Reidel, Boston) pp. 43–56.
[6] Odutola, J. A., Hu, T. A., Prinslow, D., O'dell, S. E., and Dyke, T. R., 1988, *J. chem. Phys.*, **88**, 5352.
[7] Martinache, L., Jans-Bürli, S., Vogelsanger, B., Kresa, W., and Bauder, A., 1988, *Chem. Phys. Lett.*, **149**, 424.
[8] Fraser, G. T., Suenram, R. D., and Coudert, L. H., 1989, *J. chem. Phys.*, **90**, 6077.
[9] Suenram, R. D., Fraser, G. T., and Lovas, F. J., 1989, *J. molec. Spectrosc.*, **138**, 440. Typographical errors exist in table 1 of this reference. The transitions at 66313·13, 64000·45, and 74852·29 MHz should be labelled as $B_1^{\pm}6_{06} \leftarrow 5_{05}$, $A_1^{\pm}6_{06} \leftarrow 5_{05}$, and $B_1^{\pm}7_{07} \leftarrow 6_{06}$, respectively.
[10] Hu, T. A., and Dyke, T. R., 1989, *J. chem. Phys.*, **91**, 7348.

[11] FRASER, G. T., SUENRAM, R. D., COUDERT, L. H., and FRYE, R. S., 1989, *J. molec. Spectrosc.*, **137,** 244.
[12] FRASER, G. T., 1991, *Int. Rev. phys. Chem.*, **10,** 189.
[13] BUSAROW, K. L., COHEN, R. C., BLAKE, G. A., LAUGHLIN, K. B., LEE, Y. T. and SAYKALLY, R. J., 1989, *J. chem. Phys.*, **90,** 3937.
[14] ZWART, E., TER MEULEN, J. J., and MEERTS, W. L., 1990, *Chem. Phys. Lett.*, **166,** 500.
[15] ZWART, E., TER MEULEN, J. J., and MEERTS, W. L., 1990, *Chem. Phys. Lett.*, **173,** 115. Their expression for $\bar{\nu}$ should read $\bar{\nu} = 3(A - B) + |2h_{2v}|$. Use of this expression with their data gives $A = 125{\cdot}8$ GHz.
[16] PUGLIANO, N., and SAYKALLY, R. J., 1992, *J. chem. Phys.*, **96,** 1832.
[17] HUANG, Z. S., and MILLER, R. E., 1988, *J. chem. Phys.*, **88,** 8008.
[18] HUANG, Z. S., and MILLER, R. E., 1989, *J. chem. Phys.*, **91,** 6613.
[19] DYKE, T. R., 1977, *J. chem. Phys.*, **66,** 492.
[20] HOUGEN, J. T., 1985, *J. molec. Spectrosc.*, **114,** 395.
[21] NELSON, JR. D. D., and KLEMPERER, W., 1987, *J. chem. Phys.*, **87,** 139.
[22] COUDERT, L. H., and HOUGEN, J. T., 1988, *J. molec. Spectrosc.*, **130,** 86.
[23] SMITH, B. J., SWANTON, D. J., POPLE, J. A., SCHAEFER III, H. F., and RADOM, L., 1990, *J. chem. Phys.*, **92,** 1240.
[24] COUDERT, L. H. and HOUGEN, J. T., 1990, *J. molec. Spectrosc.*, **139,** 259.
[25] GOUGH, T. E., MILLER, R. E., and SCOLES, G., 1977, *Appl. Phys. Lett.*, **30,** 338.
[26] PICKETT, H. M., 1980, *Appl. Opt.*, **19,** 2745.
[27] ALEHKIN, YU. I., ALTSHULLER, G. M., PAVLOVSKY, O. P., KARYAKIN, E. N., KRUPNOV, A. F., PAVELIEV, D. G., and SHKAEV, A. P., 1990 *Int. J. of Infrared and Millimeter Waves*, **11,** 961.
[28] KARYAKIN, E. N., SUENRAM, R. D., FRASER, G. T., and PATE, B., unpublished.
[29] COKER, D. F., and WATTS, R. O., 1987, *J. phys. Chem.*, **91,** 2513.
[30] FRASER, G. T., SUENRAM, R. D., LOVAS, F. J., PINE, A. S., HOUGEN, J. T., LAFFERTY, W. J., and MUENTER, J. S., 1988, *J. chem. Phys.*, **89,** 6028.
[31] PINE, A. S., LAFFERTY, W. J., and HOWARD, B. J., 1984, *J. chem. Phys.*, **81,** 2939.
[32] LAANE, J., 1970, *Appl. Spectrosc.*, **24,** 73.